Optical True Time Delay Network For Antenna Beam Steering in 5G Wireless Networks

Martí Llobet Turró and Josep Maria Panadés Blas
Degree in Engineering Physics,
Polytechnic University of Catalonia

(Dated: 4 June 2019)

Abstract—A photonic beam steering network for the feeding of a Phased Antenna Array (PAA) is presented. True Time Delays (TTD) are achieved through radio signal modulation over a multi-wavelength input which propagates over a Dispersion Compensating Fiber (DCF). Use of a Dual-Electrode Mach Zehnder Modulator (DE-MZM) in Dual Drive operation is shown to help avoid Chromatic Dispersion (CD)-induced amplitude fading through bias voltage adjustment while keeping wideband operation. We show examples of amplitude fading compensation through measures and simulations. Full 180° beam steering and 7 dB amplitude fading compensation in a 7-9 GHz band may be achieved in an 8-element PAA.

I. Introduction

Growing demand for enhanced broadband capacity has resulted in the development of Radio-over-Fiber (RoF) links, basically allowing for the direct irradiation of the RF analog signal by the antenna. Optical links provide wider bandwidth, low transmission loss, low weight and immunity to electromagnetic interference as compared with conventional coaxial analog links.[2]

Analog beamforming is a one of the main features to be deployed together with the rest of new technologies associated with 5G wireless networks. Dynamic adjustment of maximum directivity angle provides local antenna gain boost, overcoming path loss and allowing for greater coverage on a specific group of users.

The setup proposed in this paper includes both the RoF link and a Phased Array Antenna (PAA). Multiple tunable Distributed Feedback (DFB) lasers are used as the carrier frequency of an analog radiofrequency (RF) signal after multiplexation. The RF signal is modulated on each carrier frequency using a dual-electrode Mach-Zehnder modulator (DE-MZM) before going through a Dispersion Compensating Fiber (DCF). Each carrier frequency is differently delayed depending on each carrier frequency due to Chromatic Dispersion (CD). After demultiplexation each signal is fed into a PAA Element (PAAE). This produces a tunable beam pattern with the variation of the laser's wavelength as the input control.

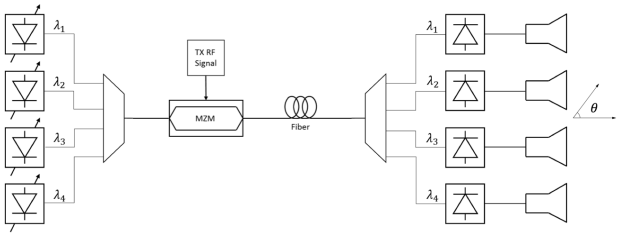

FIG. 1: Scheme for the proposed setup with 4 lasers and PAAEs

II. Characterization of a RoF link

A. Optical Carrier to Signal Ratio (OCSR)

We will assume an input electric field at the RoF link following the typical structure of the output electric field in a DE-MZM. This electric field will typically depend on the modulation index m, which will be later defined in this article. The input electric field will be:

$$E_{in} = \left(1 + \frac{m}{2}\cos\left(\omega_{RF}t\right)\right)e^{j\omega_0 t} \tag{1}$$

where ω_{RF} is the modulation frequency, which will be in the RF spectrum. The spectral power of the input electric field contains three different bands, including the carrier one at the center, and two equally displaced side bands from the center containing the signal. Total power after modulation is distributed as $P_{TOT} = P_c + 2P_{SB}$, where P_c is the carrier power and P_{SB} is the power provided by the side bands. We define the OCSR as:

$$OCSR = \frac{P_c}{2P_{SB}} \tag{2}$$

The expresion for the receveied RF signal power follows $P_{RF} = 2P_cP_{SB}$, which combining with (1) and the total power relation becomes:

$$P_{RF} = OCSR\,\frac{P_{TOT}^2}{(1+OSCR)^2} \tag{3}$$

Equation (3) shows that maximization of P_{RF} occurs for OSCR tending to 1, that is for $P_c = 2P_{SB}$. Optimization of the OCSR will be critical depending on the chosen modulation technique.

B. Amplitude fading

Ideal signal propagation assumes a linear relation between the propagation constant β and the signal's carrier frequency. Chromatic Dispersion (CD) along an optical fiber introduces a nonlinear relation, which may be mathematically represented as a Taylor expansion assuming that frequency variation of the modulated signal ($\delta\omega = \omega - \omega_0$) is negligible compared to the carrier frequency ω_0:

$$\beta(\omega) = \beta_0 + \beta_1(\omega-\omega_0) + \frac{\beta_2}{2}(\omega-\omega_0)^2 + O(\omega^3) \tag{4}$$

with

$$\beta_i = \left.\frac{\partial^i \beta}{\partial \omega^i}\right|_{\omega_0}$$

The input and output electric fields at the optical fiber may be related in the frequency domain as $E_{out}(\omega, L) = E_{in}(\omega)e^{-j\beta(\omega)L}$, where L corresponds to the fiber length. Considering an electric field at input of the optical fiber equivalent to the one at the DE-MZM output given by (1):

$$E_{out} = 1 + me^{-j\frac{\beta}{2}\omega_{RF}^2 L}\cos\omega_{RF}(t-\beta_1 L) \tag{5}$$

Experimentally we will measure the output signal in terms of its intensity detected by a photodiode $I_{ph} \propto \left|E_{out}(t,L)\right|^2$. Considering that $m \ll 1$ and applying equation (5) we may approximate output intensity as:

$$I_{ph} \approx 1 + 2m\cos\left(\frac{\beta}{2}\omega_{RF}^2 L\right)\cos\Big(\omega_{RF}(t-\beta_1 L)\Big) \tag{6}$$

We are only interested in amplitude gain, without taking into account a reference value. Intensity variation between input and output values is typically denoted S_{21} in network analyzers, defining amplitude gain G and time delay τ_g.

$$\mid S_{21} \mid = 2m\cos\left(\frac{\beta_2}{2}\omega_{RF}^2 L\right) \equiv G\cos\left(\frac{\beta_2}{2}\omega_{RF}^2 L\right) \tag{7}$$

$$\angle(S_{21}) = \omega_{RF}\beta_1 L \equiv \omega_{RF}\tau_g \tag{8}$$

Rewriting equation (6) in terms of the dispersion definition we may obtain an expression for output amplitude gain depending on the RF modulation frequency f, the dispersion coefficient D and fiber length L. In practice the effect of CD is defined with parameter D as follows:

$$D = \frac{1}{L}\left.\frac{\partial\tau_g}{\partial\lambda}\right|_{\lambda_0} \tag{9}$$

where τ_g is the time delay as seen in equation (8). Applying a change of variables via the relation for vacuum phase velocity ($c = \omega/k$) the relation of D with the β_2 parameter stated in (4) as:

$$D = -\beta_2\frac{2\pi c}{\lambda_0^2} \tag{10}$$

Combining (7) and (10) we obtain:

$$\mid S_{21} \mid = G\cos\left(\frac{\pi}{c}D\lambda_0^2 f^2 L\right) \tag{11}$$

This result denotes the existence of frequency values for which our RoF link will feature fading effects and even null-intensity points. In section IV, we will discuss how to avoid amplitude fading by the proper adjustment of the bias voltage of a Dual-Drive DE-MZM.

III. Beam steering

The frequency-dependant CD present in the DCF introduces a different time delay for each multiplexed wavelength. τ_g and CD are related locally around a certain wavelength λ_0 through (9). In the case of DCFs working with carrier wavelengths in the C-band (1530–1565 nm) we may assume a constant

value for dispersion for the entire band.[3] Relative time delay τ_g between each PAAE may then be expressed as:

$$\tau_{gi} = D\,\delta\lambda_i \tag{12}$$

with $i = 1, ..., N$, where N is the number of PAAEs. This relation will allow us to tune time delay via the adjustment of the laser carrier frequency. Different Array Factor (AF) diagrams are obtained via the use of tunable DFB lasers, slightly changing time delay between each PAAE. τ_{gi} must match the relative time delay between array elements T_s for a specific broadside direction, denoted by angle θ (see Fig 1). This relation holds $T_s = d/c\,\sin(\theta)$, where d is the PAAE interspace and c the wave velocity in vacuum. Assuming an even number of PAAEs, the corresponding wavelength shift for each laser is:

$$\delta\lambda_i = \left(i - \frac{N+1}{2}\right)\frac{T_s}{D} \tag{13}$$

The following table contains an example of possible values for a four-element PAA with a maximum directivity angle θ at 40° and −50°.

PAAE	1	2	3	4
N = 4; $\theta = 40°$				
$\delta\lambda$	118.2 nm	39.4 nm	-39.4	-118.2 nm
τ_g	-3.21 ns	-1.07 ns	1.07 ns	3.21 ns
N = 4; $\theta = -50°$				
$\delta\lambda$	-159.2 nm	-53.1 nm	53.1 nm	159.2 nm
τ_g	4.33 ns	1.44 ns	-1.44 ns	-4.33 ns

TABLE I: Required TTDs at each PAAE for a 4-element setup. Data: D = -272 ps/nm; d = 10 mm.

Introduced time delays at each PAAE depend not only on the carrier wavelength but also on the channel of the Arrayed Waveguide Grating (AWG) used for demultiplexation at the fiber output as:

$$T_{0i} = (i-1)D\,\Delta\lambda_{AWG} \equiv (i-1)T_{AWG} \tag{14}$$

where $\Delta\lambda_{AWG}$ is the AWG's channel bandwidth. Each of these delays introduced by the AWG must be compensated using with a fixed delay stage set to

$$\tau_i = (N-i)\,T_{AWG} \tag{15}$$

Implementation of these additional time delays is crucial so as to obtain the desired broadside direction of the PAA. Figure 1 contains an schematic representation of the different TTDs implemented in our setup and their relation with the available wavelengths after the AWG.

IV. Dual-Drive DE-MZM

As discussed in the previous sections, Double Side Band (DSB)-based modulation techniques introduce CD-induced amplitude fading as well as serious deterioration of link performance. Despite being DSB-based, A DE-MZM in Dual Drive operation is proposed in our setup due to its capability to avoid amplitude fading by the proper adjustment of the bias voltage while keeping wideband operation. Fading free Single Side Band (SSB)-based modulation techniques are dismissed due to their high implementation difficulty in the case that a DE-MZM is used, or due to their low flexibility in the case of optical filtering. An additional drawback for SSB modulation techniques is the 3 dB power penalty due to the suppression of one of the two sidebands in contrast to DSB modulation together with a narrower bandwidth. A detailed description of a DE-MZM in Dual Drive operation is presented in this section.[1]

A DE-MZM is a two arm optical modulator that uses an electric field to control the phase. If the contribution in each arm is properly controlled, it then becomes an intensity modulator.[4]

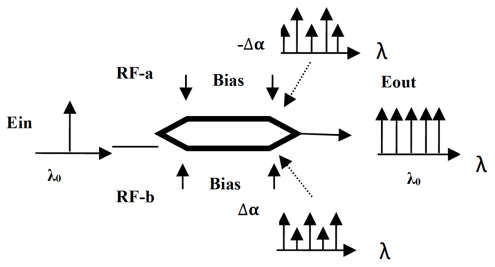

FIG. 2: Scheme of a DE-MZM in Dual Drive operation.

Two electrical signals are required in the DE-MZM, each driving the modulator at half the voltage of a single-drive device. Normal operation consists of applying half of the required electrical amplitude on each RF port, denoted RF+ and RF-,

which are dephased by factor of π.

In Figure 2, the two electrical RF signals RF-a and RF-b are applied on the two arms of the DE-MZM with two different amplitudes, along with a phase shift. These two arms are biased with -$\Delta\alpha$ and +$\Delta\alpha$ so that the amplitude can be controlled.[5]

The signal enters the modulator where an RF signal and a bias are combined and applied with different sign to each electrode, in asymmetric configuration.[6]

The electric field at the output of the DE-MZM is:

$$E_{out} = e^{j\theta_b} + e^{j\theta_{RF}} \approx e^{j\frac{\theta_b}{2}} \left(2cos\frac{\theta_b}{2} + je^{-j\frac{\theta_b}{2}}\theta_{RF} \right) \tag{16}$$

The electric field at the modulator output has been rewritten, using the following expressions, and the aforementioned parameter m:

$$\theta_{RF} = m\,cos(\omega t); \theta_b = \frac{\pi V_b}{V_\pi}; m = \frac{\pi V_{RF}}{V_\pi} \tag{17}$$

As stated before in this section, the DE-MZM in Dual Drive operation allows for the tuning of the amplitude fading profile depending on the input bias voltage. Figure 3 has been obtained using a photonic simulation software (VPI) and shows the different amplitude fading profiles in the frequency spectrum depending on the bias voltage.

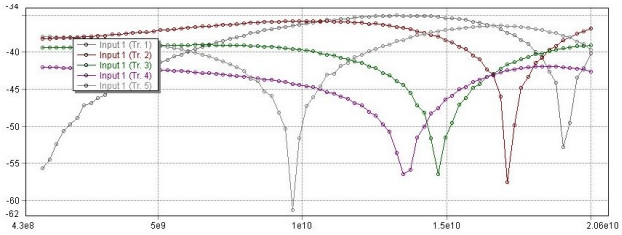

FIG. 3: Frequency spectrum of the amplitude fading profile for different bias voltages V_b at the Dual-Drive DE-MZM (horizontal axis: frequency (Hz); vertical axis: amplitude (dB)). In descending order according to the legend, the plots correspond to: $V_{b1} = 0.3V$ (Tr. 1); $V_{b2} = 0.6V$ (Tr. 2); $V_{b3} = 0.9V$ (Tr. 3); $V_{b4} = 1.2V$ (Tr. 4); $V_{b5} = 1.5V$ (Tr. 5). Additional data: D = -85 ps/(nm · km); λ = 1550 nm. Source: *VPIphotonics*.

V. Results and conclusion

The AF profiles for an 8-element PAA for modulation RFs ranging 7–9 GHz have been obtained using the VPI software. Two significant cases are included in Figure 4, denoted (i) and (ii), with applied biasings of $\theta_b = \pi/2$ (conventional biasing) and $\theta_b = -13\pi/20$, respectively. In Fig 4(i) the AF profile is negatively affected by amplitude fading, featuring a maximum power penalty of around 7 dB. This penalty increases together with the modulation RF. In Fig 4(ii) no power penalty is observed after switching to a non-conventional biasing.

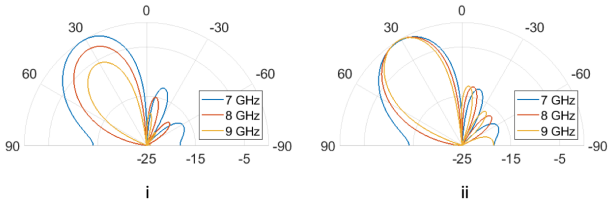

FIG. 4: Array Factor (AF) diagrams for $\theta_b = \pi/2$ (i) and $\theta_b = -13\pi/20$ (ii). Data: T_s = 23.8 ps; $\Delta\lambda_{AWG}$ = 100 GHz; D = -272 ps/nm; d = 9.4 mm. Source: *VPIphotonics*.

A full 180° beam steering may be achieved with the proposed TTD network and an 8-element PAA while avoiding CD-induced amplitude fading, as shown in Fig 4. These results hold promise for bringing into reality photonic beam steering. Together with the deployment of 5G wireless networks, quicker and more energy-efficient mobile communications are just around the corner.

References

[1] Dean P. Brown and Robert L. Nelson. *RF Performance of Single Sideband Modulation Versus Dual Sideband Modulation in a Photonic Link*. Journal of lightwave technology. 2015, pp. 1, 2.

[2] Charles Howard Cox. *Analog Optical Links*. Cambridge University Press, 2004. ISBN: 9780511324208.

[3] I. C. Goyal, A. K. Ghatak, and R. K. Varshney. "Dispersion compensating fibers". In: *Proceedings of 2002 4th International Conference on Transparent Optical Networks (IEEE Cat. No.02EX551)*. Vol. 1. Apr. 2002, 20–23 vol.1. DOI: 10.1109/ICTON.2002.1009497.

[4] Chi H. Lee. *Microwave Photonics*. CRC Press LLC, 2013, pp. 330–339. ISBN: 9781466502864.

[5] R. Nazneen and E. Zahir. "Cascading of Dual Drive Mach Zehnder Modulator and Electro Absorption Modulator for producing an optical comb". In: *2016 9th International Conference on Electrical and Computer Engineering (ICECE)*. Dec. 2016, pp. 455–458. DOI: 10.1109/ICECE.2016.7853955.

[6] Giuseppe Pecere. *Spectral Amplitude and Phase Characterization of Optical Devices by RF scan (Master Tesis)*. Master of Science in Telecommunication Engineering. Telecommunication Engineering, UPC, Barcelona. Supervisors: Maria C. Santos Blanco and Andrea Carena, 2010, pp. 49–54.